Evidence for arrested succession in a liana-infested Amazonian forest

Blaise Tymen, Maxime Réjou-Méchain, James W. Dalling, Sophie Fauset, Ted R. Feldpausch, Natalia Norden, Oliver L. Phillips, Benjamin L. Turner, Jérôme Viers, Jérôme Chave

Article:
Tymen, B, Réjou-Méchain, M, Dalling, JW et al. (7 more authors) (2016) Evidence for arrested succession in a liana-infested Amazonian forest. Journal of Ecology, 104 (1). pp. 149-159. ISSN 0022-0477

https://doi.org/10.1111/1365-2745.12504

Evidence for arrested succession in a liana-infested Amazonian forest

Blaise Tymen*[1], Maxime Réjou-Méchain[1,2], James W. Dalling[3,4], Sophie Fauset[5], Ted R. Feldpausch[5,6], Natalia Norden[7,8,9], Oliver L. Phillips[5], Benjamin L. Turner[4], Jérôme Viers[10] andJérôme Chave[1]

1- Laboratoire Evolution et Diversité Biologique UMR 5174, CNRS, Université Paul Sabatier, 118 route de Narbonne, 31062 Toulouse, France.

2- French Institute of Pondicherry, UMIFRE 21/USR 3330 CNRS-MAEE, Pondicherry, India

3- Department of Plant Biology, University of Illinois, 505 S. Goodwin Ave., Urbana, IL 61801, USA

4- Smithsonian Tropical Research Institute, Apartado 0843-03092, Balboa, Ancon, Republic of Panama

5- School of Geography, University of Leeds, University Road, Leeds LS2 9JT, UK.

6- College of Life and Environmental Sciences, University of Exeter, EX4 4RJ, UK

7- Fundación Cedrela, Diagonal 40A # 18A-09, Bogotá, Colombia

8- Centro Internacional de Física, Universidad Nacional de Colombia, Cra 30 # 45-03, Bogotá, Colombia

9- Programa de Biología, Facultad de Ciencias Naturales y Matemáticas, Universidad del Rosario, Bogotá, Colombia

10- Géosciences Environnement Toulouse UMR 5563, Université Paul Sabatier, CNRS, IRD, 14 avenue Édouard Belin 31400 Toulouse, France.

23

24 * Correspondence author. E-mail:blaise.tymen@gmail.com**Running headline:** Liana-infested

25 forests as an arrested succession stage

Summary

1. Empirical evidence and modelling both suggest that global changes may lead to an increased dominance of lianas, and thus to an increased prevalence of liana-infested forest formations in tropical forests. The implications for tropical forest structure and the carbon cycle remain poorly understood.

2. We studied the ecological processes underpinning the structure and dynamics of a liana-infested forest in French Guiana, using a combination of long-term surveys (tree, liana, seedling and litterfall), soil chemical analyses and remote sensing approaches (LiDAR and Landsat).

3. At stand scale and for adult-trees, the liana-infested forest had higher growth, recruitment, and mortality rates than the neighbouring high-canopy forest. Both total seedling density and tree seedling recruitment were lower in the liana-infested forest. Stand scale above-ground biomass of the liana-infested forest was 58% lower than in the high-canopy forest.

4. Above-ground net primary productivity (ANPP) was comparable in the liana-infested and high-canopy forests. However, due to more abundant leaf production, the relative contribution of fast turnover carbon pools to ANPP was larger in the liana-infested forest and the carbon residence time was half that of the high-canopy forest.

5. Although soils of the liana-infested forest were richer in nutrients, soil elemental ratios suggest that liana-infested forest and high-canopy forest soils both derive from the same geological substrate. The higher nutrient concentration in the liana-infested forest may therefore be the result of a release of nutrients from vegetation after a forest blow down.

6. Using small-footprint LiDAR campaigns, we show that the overall extent of the liana-infested forest has remained stable from 2007 to 2012 but about 10% of the forest area changed in forest cover type. Landsat optical imagery confirms the liana-infested forest presence in the landscape for at least 25 years.

7. Synthesis: Because persistently high rates of liana infestation are maintained by the fast dynamics of the liana-infested forest, liana-infested forests here appear to be the result of an arrested tropical forest succession. If the prevalence of such arrested succession forests were to increase in the future, this would have important implications for the carbon sink potential of Amazonian forests.

Key words: Above-ground productivity; Biomass; Carbon turnover; Determinants of plant community diversity and structure; Forest dynamics; Forest structure; French Guiana; Remote sensing.

Introduction

Lianas are an ecologically important plant functional group in tropical forests. They constitute less than 10% of the forest above-ground biomass (Putz 1984a; DeWalt & Chave 2004), but represent a significant share of the plant taxonomic diversity (Gentry 1988; Schnitzer et al. 2012) and they also play an important role in tropical forest ecosystem functioning (Wright et al. 2004; Schnitzer, Bongers & Wright 2011). For instance, they represent up to 40% of leaf net primary productivity in some forests (Putz 1983). Lianas may be favoured competitively by the increase in atmospheric CO_2 concentration (Granados & Körner 2002; Phillips et al. 2002; Wright et al. 2004), by long-term increases in tree dynamics (Phillips & Gentry 1994), and by higher potential evapotranspiration rates associated with longer and warmer dry seasons (Schnitzer 2005; Heijden & Phillips 2008; Schnitzer & Bongers 2011). Understanding the function of lianas in tropical rainforests is therefore an important challenge in community ecology and ecosystem science (Schnitzer & Bongers 2002; van der Heijden & Phillips 2009; Schnitzer et al. 2014).

Some forest areas are currently dominated by lianas (henceforth ‘liana-infested forests’) both in Central Africa and Amazonia (Caballé 1978; Pérez-Salicrup 2001). Lianas abundance

increases with forest disturbance (Schnitzer & Bongers 2011; Dalling et al. 2012). They respond to light availability faster than trees, and find more support for growth in secondary forests (Putz 1984a; Letcher & Chazdon 2012). In some large liana-infested treefall gaps, lianas have been shown to suppress the regeneration of trees (Schnitzer & Carson 2010), to the extent that liana-infested forests have been interpreted as arrested stages of ecological succession after past disturbance (Schnitzer et al. 2000; Foster, Townsend & Zganjar 2008). Alternatively, liana-infested forests could result from some localized difference in the natural environment, notably since lianas occur more frequently on more fertile soils (Schnitzer & Bongers 2002 but see Dalling et al. 2012).

However, these two scenarios are not exclusive. If a forest blow-down has occurred recently, large amounts of nutrients previously held in the living biomass should be released to the topsoil. Thus, soil nutrient content of a disturbed area may differ from that of an undisturbed forest on the same geological substrate. Unravelling causal factors in the establishment of a liana-infested forest is therefore a challenging task.

In the present study, we seek to identify the ecological mechanisms underpinning the origin and the maintenance of liana-infested forests. To do so, we combine data on a liana-infested forest patch of about 20ha from repeated field censuses of seedlings, long-term monitoring of trees and lianas, extensive soil chemical analyses, litterfall surveys, and repeated airborne LiDAR coverage and Landsat data. Because of competition, we expect a negative correlation between liana infestation and tree growth and survival (Clark & Clark 1990; van der Heijden & Phillips 2009; Ingwell et al. 2010). Litterfall rate is expected to be greater in the liana-infested forest than in the high-canopy forest because lianas allocate proportionally more resources to leaves (van der Sande et al. 2013). Also, we expect that liana-infested forests to be more fertile than the neighboring high-canopy forests. However, we propose to test whether these differences in soil fertility are caused by the underlying substrate or by disturbance history. Finally, we expect that the spatial extension of the liana-infested forest has remained stable over the past years if it was an arrested stage of succession.

Material and Methods

STUDY SITE

The study site is a 136-ha area within the old-growth tropical moist forest of the Nouragues Ecological Research Station, in central French Guiana, located ca. 100 km south of Cayenne (Latitude: 4° 04' 27.986" N, Longitude: 52° 40' 45.107" W). The area is part of the Nouragues Natural Reserve, within a zone delineated for scientific research. The terrain is gently rolling with small hills and with an elevation ranging between 50 and 175 m asl. Annual rainfall is typical of equatorial evergreen tropical forests with 2861 mm $year^{-1}$ (1992-2012 average) with a two months dry season (precipitation below 100 mm $month^{-1}$) in September and October. High-canopy forest, liana-infested forest and bamboo thickets are the three main vegetation types in the study area (Réjou-Méchain et al. under revision). The Nouragues forest shows no obvious evidence of recent anthropogenic disturbances. The presence of an Amerindian tribe consisting of less than 1000 people, called 'Nouragues' was noted in the region by maps of the 17th century, and most notably by the writing of two priests of the Company of Jesus, Jean Grillet and François-Jean Béchamel (Béchamel 1682; Coudreau 1893). Human presence is also attested by the discovery of artefacts found in the vicinity of the scientific camp (Bongers et al. 2001). However, the study area is remote from a major river tributary (15 km as the crow flies from the Approuague river), and neither the soil nor the topography are particularly suitable for slash-and-burn agriculture. The Nouragues Amerindians had departed the area and moved further south by the mid-18th century. Subsequent scattered human presence occurred during the 19th and 20th centuries (gold rushes, latex harvesting of the 'balata' tree, *Manilkara* spp.) but these were limited in scale and concerned mostly the more accessible areas surrounding major river tributaries. For instance, *Manilkara* trees show no evidence of past exploitation in or nearby our study area.

FOREST STRUCTURE AND DYNAMICS

124 The liana-infested forest is spatially localized and characterized by a high density of small lianas
125 and a large number of leaning and slanting trees. It is also characterized by a lower canopy height.
126 To compare the dynamics of the high-canopy forest and the liana-infested forest we relied on three
127 datasets collected in the field: (i) long-term inventory for trees and lianas ≥ 10 cm in diameter at
128 breast height (DBH); (ii) long-term inventory of seedlings ≤ 1 cm in diameter; (iii) quantification of
129 litterfall using permanent collecting traps, regularly emptied and dried.

130 A large permanent sample plot of 10ha (1000 x 100 m²) was established in 1993 to study the
131 transition from high-canopy forest to the liana-infested forest (Chave, Riéra & Dubois 2001; Chave
132 et al. 2008). All trees and lianas ≥ 10 cm DBH were measured and mapped. The plot was re-
133 censused for trees and lianas in 2000, then again in 2008 and 2012, following the RAINFOR
134 protocol (Phillips et al. 2010). During the 2008 census, plot limits were corrected, and all points of
135 measurement (POM) were marked with a paint line, allowing a more accurate measurement of tree
136 growth between 2008 and 2012. The diameter of stilt-rooted or buttressed trees was measured 50
137 cm above the last root or buttress. Trees and lianas were individually tagged. In 1992 and 2000,
138 liana diameters were measured at 130 cm above-ground. In 2008 and 2012, they were measured at
139 four points following the recommendations of Schnitzer, DeWalt & Chave (2006): (1) the largest
140 point on the stem, devoid of such stem abnormalities as large growths, knots, fissures, or wounds;
141 (2) 20 cm along the stem from the last substantial root; (3) 130 cm from the last substantial root;
142 and (4) 130 cm above-ground (DBH). Data are available from the ForestPlots.net online database
143 (http://www. forestplots. net/ - accessed 13 June 2013; Lopez-Gonzalez et al. 2011). For each liana
144 with DBH ≥ 10 cm, hereafter referred to as large lianas, the host tree was recorded and referred to
145 as an infested tree (possibly several trees were the hosts of one liana). We note that trees were
146 frequently infested by smaller lianas, so our estimate of infested trees is conservative.

147 To address potential underestimation of liana infestation, a quantification of the liana leaves
148 in tree crowns was performed during the 2012 field campaign through the use of the crown
149 occupation index (COI) (Clark & Clark 1990). This index ranks trees from 0 to 4 according to the

infestation rate of their crown: (0) no lianas leaves in the crown, (1) 1–25%, (2) 26–50%, (3) 51–75%, and (4) >75% of the tree crown covered by liana leaves (Appendix S1). This index of liana infestation has been shown to be accurate and repeatable at individual and plot levels (van der Heijden et al. 2010).

Annual trunk diameter growth rate for census i (g_i in cm year^{-1}) was computed for each tree from the DBH measurements assuming a constant growth during the census interval. Population demographic parameters were computed in 25x25-m² subplots. Mortality rate (M_i in year^{-1}) was calculated as proposed by Sheil & May (1996): $M_i = -\frac{1}{\Delta t}\ln(\frac{N_i - N_{ri}}{N_{i-1}})$ with N_i being the number of trees in the census i, Δt the time interval between the two censuses, and N_{ri} the number of recruits between censuses i-1 and i. Likewise, annual recruitment (K_i in tree per hectare) was computed using the following equation (Sheil & May 1996): $K_i = M_i N_{ri}/A(1 - e^{-M_i \Delta t})$ with N_{ri} the number of recruits at time t_i, A the plot area (in ha), and M the mortality rate. To facilitate comparison among forest types that differed in stem density, we reported annual recruitment in % year^{-1} (see Table 1).

Tree and liana seedlings were monitored in 250 plots of 1x1m² established in cluster of 2-3 plots in 100 regularly spaced locations (Fig. 1c, Norden et al. 2007, 2009). Each seedling plot was censused at least four times between 2004 and 2013 except three of them which were removed from the analyses because they experienced treefall or other problems. During each census, recruits were counted, identified whenever possible and measured. Overall, 19.5 % of the seedlings were identified as lianas and 58.2 % as trees. The rest could not be identified with confidence. Mortality and recruitment rates of seedlings were large and therefore we didn't make the assumptions made for trees and estimated these rates from empirical data as follows. Seedling mortality rate (m_i in year^{-1}) at census i was quantified as: $\ln(1 - m_i) = \frac{1}{\Delta t}\ln(\frac{N_i - N_{ri}}{N_{i-1}})$ and seedling recruitment (in m^{-2}year^{-1}) as $k_i = \frac{m_i N_{ri}}{A - A(1-m_i)^{\Delta t}}$, with N_{ri} being again the number of recruits at time t_i and $\Delta t = t_i - t_{i-1}$ in years. We then averaged the rates to obtain a 9-year average at each location (2 to 3 plots per

location). These analyses were performed for tree and liana separately and also for all seedlings together (including undetermined).

Litterfall was collected from 100 0.5-m^2 litter traps at the seedling plots locations (Fig. 1.c, Chave et al. 2008, 2010). From February 2001 to February 2003, these traps were collected twice monthly, their content separated into leaves, twigs, flowers and fruits, and the fractions oven-dried and weighed. We contrasted total litterfall and its fractions (leaf, twigs, and reproductive organs) between the high-canopy forest and the liana-infested forest.

Tree above-ground biomass (AGB) was estimated using a pantropical biomass equation (eq. 4 in Chave et al. 2014) combined with locally-adjusted height-diameter models (Réjou-Méchain et al. under revision). Liana AGB was computed using the allometric equations from Schnitzer et al. (2006) using the diameter measured at 130 cm from the last substantial root when available (2008 and 2012 censuses) or the diameter measured at 130 cm above-ground (1992 and 200 censuses). Above-ground net primary productivity (ANPP) was computed as the AGB stock increment induced by recruitment and growth of trees with DBH $\geq$ 10 cm plus total litterfall production. Other ANPP components, although they may be important (Clark et al. 2001) were not considered in the present study. Residence time of carbon in the above-ground vegetation was computed as the ratio AGB/ANPP.

AIRBORNE DATA ACQUISITION, PROCESSING, AND ANALYSES

Two airborne LiDAR acquisitions were conducted in 2007 and 2012 by a private contractor (http://www.altoa.fr/, for more details see Appendix S4). LiDAR datasets consisted of a cloud of laser echoes originating from ground and vegetation. Ground points were identified using the TerraScan (TerraSolid, Helsinki) 'Ground' routine'. Based on this dataset, we constructed a 1-m resolution elevation model using the "GridSurfaceCreate" procedure implemented in FUSION (McGaughey 2009).

For both 2007 and 2012 cloud point datasets, 1-m and 5-m canopy models were built after outlier extraction, using the "CanopyModel" procedure implemented in FUSION. This procedure subtracts the elevation model from the height of each return and then uses the highest return value to compute the canopy surface model. A 3x3 cell median filter was applied to smooth the surface and avoid local unrealistic maxima

In our study zone, large areas of known liana-infested forest formations had a canopy height typically ranging between 10 and 20 m, while surrounding forests had a significantly taller canopy (25 to 35 m). Thus, we used the LiDAR canopy model to identify all pixels having a top-of-canopy height comprised between 10 and 20 m and connected to the known liana-infested forests patches. These low-canopy pixels were considered as liana-infested. A 5-m buffer around the liana-infested forest class was also assigned to the liana-infested forest class, and pixels entirely surrounded by liana-infested forest were included in it. In a second step, this forest classification was validated using ground truthing and aerial photographs and was found to be highly accurate (Fig. 1; Appendix S1). Next, we defined a 50-m transition zone surrounding the liana-infested zone (Fig. 1); this zone was removed from the analyses because we assumed it to be influenced by both forest types. Finally, we removed the area covered by a 1-ha bamboo thicket and a 30-m buffer zone around it (total of 2.7ha, Fig. 1). Aerial photographs of the study site were taken in 2008 (Fig. 1). They were used to qualitatively check the accuracy of our delineation of the liana zone and bamboo thickets.

LiDAR-derived variables were assessed within a 50x50-m² grid based on the 1-m resolution LiDAR canopy model. Gaps were defined as areas where canopy elevation was lower than 5 m, a convention similar to that in Hubbell et al. (1999). We did not define any minimal area for such gaps; tree-fall gaps, branch-fall gaps and other openings in the canopy are thus included in our definition of gap. From the canopy height distribution, mean and coefficient of variation (standard deviation divided by the mean) were computed within each 50x50-m² grid cell. Grids cells were assigned to the different vegetation types (liana-infested forest, transition zone, high-canopy forest) when at least 50% of the grid area contained the vegetation.

SOIL CHEMICAL ANALYSES

We first tested if the soil of the liana-infested forest was more fertile than the high-canopy forest soil. To do so, we used two different datasets. The first dataset was collected as part of a previous project aiming to assess the influence of environment on seedling dynamics (Norden et al. 2007, 2009). A total of 100 soil samples were collected in the study area and analyzed (Fig. 1.c). Of these, eight soil samples came from the liana-infested forest and 62 from the high-canopy forest; 30 samples from the transition zone were removed from the analysis. Topsoil (0-10 cm depth) was filtered in a 2-mm mesh sieve after removing litter and was then acid-digested. Total concentrations of major elements were measured by inductively coupled plasma optical emission spectroscopy (ICP-OES). In addition, concentrations of carbon and nitrogen were measured by a CHN elemental analyzer (NA 2100 Protein, CE Instruments®) and soil pH was measured in a standard solution made up of one volume of soil diluted in three volumes of water (Norden et al. 2009). The second dataset was collected in 2011 and included seven soil samples from the liana-infested forest and 21 from the high-canopy forest; 12 samples from the transition zone were removed from the analysis (JWD and BLT, unpublished results). Exchangeable cations were measured, and metals were extracted in 0.1 M $BaCl_2$ solution in a 1:30 soil to solution ratio for 2 hours. Detection was performed by inductively-coupled plasma optical-emission spectrometry on an Optima 7300 DV (Perkin-Elmer Ltd, Shelton, CT; Hendershot, Lalande & Duquette 1993; Schwertfeger & Hendershot 2009). Total exchangeable bases (TEB) were calculated as the sum of the concentrations of Ca, K, Mg and Na; effective cation exchange capacity (ECEC) was calculated as the sum of Al, Ca, Mg, Mn, H and Na. Base saturation (BS, %), a measure of soil cation fertility was calculated as: $BS = \frac{100 \times ECEC}{TEB}$. Exchangeable phosphorus concentration was measured by adsorption on anion-exchange resins (Turner & Romero 2009).

For both datasets, a principal component analysis (PCA) was performed on concentration values (mg kg^{-1} of soil). Sample scores on the PCA axes were compared between high-canopy forest and liana-infested forest soils.

We then tested whether the occurrence of the liana-infested forest is related to the nature of the bedrock. We analyzed the concentration of a range of rare elements in the soil that are tracers of substrate heterogeneity at the site. Geochemical tracers are now commonly used to distinguish the nature of rocks, the origin of sediments or sedimentary recycling processes (McLennan et al. 1993; Lahtinen 2000) because they are sensitive to chemical reactions over geological timescales (McLennan et al. 1993). Ratios of some of these tracers are useful to explore substrate homogeneity since they are conserved between the source (rock) and the weathered product (soil). We collected surface soil samples with an auger at six sites, two within the liana forest, and four in the high-canopy forest (Fig. 1). To measure the elemental concentrations, all samples were digested by acid attack in Teflon Savillex® vessels. We also digested the samples by alkali fusion to check that all refractory minerals have been dissolved during the acid attack digestion. In both procedures, a GA standard (granite, CRPG-CNRS Nancy, France) was included in the analyses for control. Trace elements were analyzed on an ICP-MS (7500 ce, Agilent Technologies). After calibration, the certified reference materials (SLRS-5, NRCC, Canada and ION-915, Environment Canada), together with the GA standard, were analyzed to assess the validity and the reproducibility of the procedure. We then calculated the chemical ratios at all six sites (see Appendix S2 for further information). Ratios analyzed here are: Cr/Th, Cr/V, Zr/Y and Eu/Eu*, with $Eu^* = \frac{Eu}{Eu_{ref}} \times \frac{Sm_{ref}}{Sm} \times \sqrt{\frac{Tb_{ref}}{Tb}}$ (McLennan et al. 1993).

LANDSAT DATA PROCESSING AND ANALYSES

Cloud-free 30-m resolution Landsat Thematic Mapper (TM) data were rare in the study area. We found three high-quality images, acquired on 18 July 1988, 24 July 1990 and 8 October 2006. Geo-

referencing of the Landsat images was adjusted using the LiDAR data in Qgis 2.2-Valmiera. Radiometric corrections were applied to the 1990 and 1988 data relatively to the 2006 data using the histogram matching algorithm implemented in the 'landsat' R package.

We characterized the pixels of Landsat images using the tasseled-cap indices (Crist & Cicone 1984). These indices are commonly used because they are scene-invariant and summarize vegetation characteristics: brightness, greenness and wetness and were used in a previous study on liana-infested patches (Foster et al. 2008). Before any classification, a low-pass filter was applied on all three Landsat images to reduce their variance following Hill (1999). Pixels of the modified 2006 Landsat image were classified as belonging to the liana-infested forest or not using the area identified with the 2007 LiDAR dataset (see above). A Principal Component Analysis (PCA) was then performed on the tasseled-cap indices values of the 2006 image (Fig. S3). To allow direct comparisons between images, the PCA scores of the pixels from the 1988 and 1990 images were calculated using the scalar product associated to the row weightings of the PCA performed on the 2006 image (function 'suprow' in ade4 R package). A hierarchical classification following Ward's method was performed based on the pixel's scores of the two first PCA axes. Classes of this unsupervised method were mapped and compared to the liana-infested forest defined based on LiDAR data.

All statistical analyses were performed with the R statistical software v3.1.1 (R Core Team 2012). Raster manipulation, spatial analyses, and hierarchical clustering were performed using the 'raster', 'maptools', 'sp', 'fields' and 'ade4' packages in R.

Results

IMPACT OF LIANA INFESTATION ON FOREST STAND STRUCTURE AND DYNAMICS

We first compared the stand structure parameters (Table 1). We found no significant difference in tree stem density within and outside of the liana-infested forest (Wilcoxon test, P=0.78); however,

297 mean stand-level basal area of trees was 50% lower and above-ground biomass (AGB) stock 58%
298 lower in the liana-infested forest than in the high-canopy forest (Fig. S2, Table 1). Liana AGB was
299 slightly higher in the liana-infested forest. The liana-infested forest canopy was also more irregular
300 with five times more canopy gaps (Fig. 2).

301 Next, we contrasted stand dynamics parameters (Table 1). Both recruitment and mortality
302 rates of trees >10 cm DBH were more than twice as high in the liana-infested forest as outside of it.
303 Over the 1992-2012 period, the liana-infested forest lost biomass carbon with its AGB stock
304 dropping from 185 ± 21 $Mg.ha^{-1}$ in 1992 to 163 ± 22 $Mg.ha^{-1}$ in 2012. Conversely, during the same
305 period, the high-canopy forest gained biomass carbon with its AGB stock increasing from 386 ±
306 21$Mg.ha^{-1}$ in 1992 to 438 ± 29 $Mg.ha^{-1}$ in 2012 (Fig. S7). In contrast, the increase in liana AGB was
307 1.5 times higher in the liana-infested forest than in the surrounding forest (Table 1).

308 Litterfall production was higher in the liana-infested forest than in the high-canopy forest
309 (Table 1). The difference was due to leaf fall, which represented about 70% of the litterfall, while
310 fruit and flower falls were higher in the high-canopy forest. However, above-ground net primary
311 productivity (ANPP) was comparable between the liana-infested forest and the high-canopy forest.
312 Owing to a lower AGB stock, the estimated residence time of carbon (i.e. the ratio of AGB to
313 ANPP) in the liana-infested forest was therefore half that of the high-canopy forest.

314 Seedling mortality was consistently higher in the liana forest than in the high-canopy forest
315 without detectable difference between lianas and trees (Table 2). However, unlike adult tree
316 recruitment, tree seedling recruitment was lower in the liana forest while liana-seedling recruitment
317 was similar in both forest types. Of the identified seedling recruits, 45% were lianas in the liana-
318 infested forest versus 25% in the surrounding high-canopy forest.

319 SOIL CHEMISTRY IN THE LIANA-INFESTED FOREST

320 Soil chemistry differed substantially between the liana-infested and high-canopy forest (Table 3).
321 For total nutrients extracted from surface soils, liana-infested forest samples had significantly

different PCA scores than sample from the high-canopy forest (Wilcoxon test, p=0.001 for the two first axes, Fig. S5). In the liana-infested area, surface soil was richer in macro-elements (C, Ca, K, Mg, and N) and had a higher pH than in the high-canopy area (Table 3). In addition, soil samples from the liana-infested forest had different scores than the high-canopy forest on the first axis of the PCA (Wilcoxon test, p=0.036, Table 3¸ and Fig. S6). Base saturation was higher in the liana-infested forest than in the high-canopy forest (Wilcoxon test, p=0.027, Table 3).

According to trace elements ratios, the underlying substrate of the Nouragues forest was typical of comparable substrates of the Guiana Shield (Fig. 3 and Appendix S3, Table S1). The samples from the liana-infested forest did not differ from those collected in the surrounding high-canopy forest (Fig. 3 & S4). These results suggest that the soils within and outside of the liana-infested forest most likely derive from a similar lithology.

CHANGES IN THE SPATIAL FOOTPRINT OF THE LIANA-INFESTED FOREST

Between 2007 and 2012, the liana-infested area declined by 3.4%, from 23.6 ha to 22.8 ha. In total, 21.1 ha (89.5%) remained in the liana-infested forest class while 2.5 ha (10.5%) was grown over by tall trees, and 1.7 ha was recruited as new liana-infested forest (7.5% of the 2012 liana-infested forest). Losses of liana-infested areas were due to trees outgrowing the height threshold, while gains were due to additional tree falls in the liana-infested transition area.

The unsupervised segmentation of the Landsat 2006 image produced a forest classification where a single class showed a good agreement with the liana-infested area as delineated by the 2007 LiDAR dataset (Fig. 4 & S3). The liana-infested forest was characterized by higher greenness and brightness indices and by a lower wetness index based on tasseled-cap indices (Fig. S3). Over 68% of the liana-infested forest was classified as liana-infested forest type either in the 1988 or in the 1990 Landsat scenes. Our analysis indicates a fair degree of stability of the liana-infested forest for at least 25 years (Fig. 4).

Discussion

Long-term forest monitoring allowed a detailed analysis of the structure, dynamics, and above-ground net production of a naturally liana-infested tropical formation. At stand level, liana infestation was associated with faster forest dynamics, both in terms of demography and of carbon turnover. Soils in the liana-infested forest were nutrient-poor by Amazonian standards but they were richer in nutrients than high-canopy forest soils. However, the underlying substrates were not detectably different in their chemical composition. Finally, the extent of the liana-infested area was found to be fairly stable over at least the past 25 years. Overall, these results suggest that the liana-infested forest is in an arrested stage of ecological succession. Below, we discuss evidence for this claim and its implications.

INFLUENCE OF LIANAS ON FOREST DYNAMICS

We found that lianas have a profound impact on the stand-level dynamics of the liana-infested forest. They induced a faster tree dynamics than in the surrounding high-canopy forest. This was probably due to a greater proportion of fast-growing, high-mortality tree species, which are better at shedding and avoiding lianas(Putz 1984b; Schnitzer & Bongers 2002). Thus, direct competition between trees and lianas probably had a strong influence in favouring the high-turnover dynamics. Because of high tree mortality rate, we also observed more frequent gap openings which is expected to favour liana maintenance and establishment (Dalling et al. 2012; Ledo & Schnitzer 2014).

The liana-infested forest stored 2.4 times less AGB than in the high-canopy forest, a figure comparable to that described by Schnitzer et al (2014) who compared liana-infested and liana-free tree gaps. However, ANPP in the liana-infested forest was similar to that of the surrounding high-canopy forest, in spite of the very different structure and biomass. Also, litterfall production was slightly higher in the liana-infested than in the surrounding high-canopy forest and was greater than typical values for both secondary and old-growth forests (Chave et al. 2010). This was presumably due to a greater allocation of resources to leaves in lianas than in trees. As a result, carbon residence

time in the liana-infested forest was half that of the high-canopy forest. At global scales, carbon residence time is strongly controlled by climate (Carvalhais et al. 2014). Yet our findings demonstrate that at landscape scale the biological composition and structure of forests is a strong determinant of carbon residence times in agreement with Malhi et al. (2004).

We were able to study the differential regeneration of trees and lianas in the liana-infested forest, and we found a relative advantage of liana over tree seedlings. This suggests that liana regeneration is promoted in the liana-infested forest environment, either through higher seed availability or more suitable habitat for germination and seedling establishment. In contrast, tree seedling recruitment was lower than liana seedling recruitment in the liana-infested forest (Table 2). This may either be due to lower seed arrival rates, lower seed germination, or to early seedling mortality (i.e. occurring between germination and the census date). In liana-infested tree-fall gaps, Schnitzer & Carson (2010) showed a high seedling recruitment limitation for shade-tolerant tree species but not for pioneer species. We expect the same effect in the Nouragues liana-infested forest and predict that liana infestation should enhance the recruitment of pioneer tree species thus maintaining high forest turnover (Schnitzer & Bongers 2002). However, we were unable to assess this prediction quantitatively, because too few seedlings were identified to species in our dataset.

We also found that total seedling mortality was higher in the liana-infested forest. Consistently, Norden et al. (2007) found lower seedling survival in sites with higher light availability and higher soil fertility, some conditions met in liana-infested forest as shown in our study. They interpreted this pattern as the consequence of a more intense competition in resource-rich environments. However, higher seedling mortality in the liana-infested forest could also result from the higher leaf litterfall because leaf litter cover seedling and hence lowers their emergence and increase their mortality (Guzman-Grajales & Walker 1991; Dalling & Hubbell 2002)

THE LIANA-INFESTED FOREST AS AN ARRESTED STAGE OF SUCCESSION

A most remarkable feature at Nouragues is that the liana-infested forest appears to be an arrested stage of ecological succession. LiDAR surveys revealed that the liana-infested forest was spatially stable during a five-year interval, with no notable net gain or loss over the surrounding high-canopy forest. This result was extended by an analysis of long-term Landsat series, starting in 1988, and by previous observations by Sabatier & Prévost who mentioned the presence of a liana-infested forest with similar location in 1987and suggested considering this formation as 'homeostatic' (Sabatier & Prévost 1990). The well-documented spatial stability of the liana-infested forest at Nouragues now provides solid evidence that such forest formations can persist for decades with no apparent evidence of transition towards a different structural state.

One possible explanation for the apparent stability of the liana-dominated forest could be the association of lianas with more fertile soils as found in Asian tropical forests (reviewed in Schnitzer & Bongers 2002). We confirmed that soil in the liana-infested forest was more fertile with higher base saturation and phosphorus than the surrounding forest (Sollins 1998; Phillips et al. 2003; Tuomisto et al. 2003). Because the liana-infested forest has lower AGB, and therefore less nutrient quantities stored in live organs, the amount of nutrients available in the soil would be higher if the soil had the same characteristics. Higher base saturation of the soil in the liana-infested forest than in the high-canopy forest would then be due to differences in forest structure rather than differences in rock weathering.

To disentangle the relative role of rock substrate and above-ground versus below-ground nutrient storage, we used geological tracers that are typical of substrate type but are not strongly affected by the biochemical cycling over ecological time scales. While there are differences in chemical element contents, tracer ratios, supposed to be more stable through pedogenesis, did not reveal striking differences in the lithology from which the soils derive through weathering (Fig. 3 & Supplementary Information 2). The similar bedrock chemical composition within and without the liana-infested forest shown by tracer analyses suggest that geology is not a causal factor for liana dominance in the study zone.

Overall, our results support the hypothesis of a release of nutrients into the soil due to a past disturbance and maintained by the fast vegetation turnover of the liana-infested forest. Such disturbance may have been either natural (i.e., convectional storm) or human-mediated (i.e., human settlement). The size of the area, its location, and previous knowledge on human settlements in this area all suggest that a human cause is less likely. Surveys found no human artefacts (pottery or charcoal) in the liana-infested forest (B. Hérault, M. van der Bel, S. Barthe, unpublished results). A few years ago, a blow-down of a similar size caused by a micro-tornado was discovered a few km north of the study area (C. Bienaimé, P. Gaucher, pers. comm.). A similar event may have also triggered the establishment of our liana-infested forest. After the completion of this manuscript it has come to our attention that a study conducted in the Imataca Forest Reserve in Eastern Venezuela has proposed the same hypothesis for the origin of a local liana-infested forest (Lozada et al. 2015).

Our analysis focuses on a single patch of liana forest, and therefore lacks replication. It would be useful to compare the dynamics of the liana-infested forest as reported in this study with that of other liana-dominated formations of similar sizes in other parts of the Amazon. However we suspect that many of our findings are likely to extend beyond our study site. In particular, as discussed above, we suspect that the ability of lianas to significantly slow down ecological succession will hold at other sites. Alternative pathways of treefall gap regeneration caused by liana infestation have already been detected at Barro Colorado Island in Panama. Schnitzer et al. (2000) and Schnitzer & Carson (2010) have shown that liana density was positively correlated with pioneer tree density and that canopy height remained low for over 13 years in those gaps. Foster et al. (2008) also showed that liana-infested forests demonstrated that liana-infested patches did not recover even after 14 years, and may therefore be considered as an arrested succession in the Noel Kempff Mercado National Park in eastern Bolivia. Also, it is likely that nutrient-rich soils in liana formations generally are a consequence of pre-liana disturbance rather than be associated to geomorphology. Finally, we believe the disturbance event that resulted in lianas overtaking this area

was not directly related to human occupation. It seems that other liana-dominated forests are of non-anthropogenic origin in the Amazon, but human-induced disturbances are expected to favour lianas infestation (Schnitzer & Bongers 2011). It would be important to better document the extent and origins of liana-infested forests at a regional scale. We conclude by discussing the possible implications of liana dominance at regional scale.

REGIONAL-SCALE IMPLICATIONS OF LIANA DOMINANCE

Our results confirm that liana infestation limits the net carbon sequestration capacity of tropical forests (Phillips et al. 2002; van der Heijden et al. 2013; Schnitzer et al. 2014). Lianas have already been found to have increased over recent decades in dominance even in undisturbed Neotropical forests, possibly due to climate or atmospheric changes (Phillips et al. 2002; Laurance et al. 2014). Lianas may also be expected to benefit in coming decades, if tree mortality rates continue to rise (Brienen et al. 2015), and/or if disturbances at regional scale become more frequent because of warming, leading potentially to more frequent extreme events (Davidson et al. 2012). These phenomena could favour the emergence of larger areas of liana-infested forest. Importantly, the transition rate from high-canopy to liana-dominated forests has been understudied, since it is difficult to monitor vast expanses of tropical forest as the appropriate spatial resolution (only one study from Foster et al. 2008). Larger-scale airborne LiDAR surveys combined with the development of new satellite Earth observation technologies may radically transform our vision for this problem. We would be able to provide a much finer-grained detail of the canopy structure and dynamics and potentially directly detect the influence of liana infestation.

Currently, evidence for forest regeneration following deforestation suggests that tropical forests rapidly accumulate carbon during the early stages of regeneration (Brown & Lugo 1990). Typically, for forests growing in the conditions met in our study site, a recovery of 85% of the carbon stock contained in the initial old-growth forest is expected in about 80 year thanks to a carbon accumulation rate close to 5 $Mg.ha^{-1}.year^{-1}$ (Bonner et al. 2013). By contrast, in the liana-

infested forest we studied, carbon stock remained stable at c.a. 40% of the high-canopy forest carbon stock over the past 20 years (Fig.S7). The finding that tropical forests may turn into low-AGB forests for decades is a cautionary tale for carbon cycle modellers because it could have a dramatic impact on the carbon storage ability of these forests in the future as it was already pointed out by van der Heijden (2013).

Acknowledgments

We thank V. Alt, C. Baghooa, C. Baldeck, C. Baraloto, W. Bétian, V. Bézard, L. Blanc, V. Chama Moscoso, P. Châtelet, M. Delaval, J. Engel, P. Gaucher, T. Gaui, S. Icho, G. Lopez-Gonzalez, A. Monteagudo, P. Pétronelli, G. Pickavance, and J. Ricardo for field data collection and curation. We gratefully acknowledge financial support from CNES (postdoctoral grant to MRM, and TOSCA programme), and from "Investissement d'Avenir" grants managed by Agence Nationale de la Recherche (CEBA, ref. ANR-10-LABX-25-01; TULIP: ANR-10-LABX-0041; ANAEE-France: ANR-11-INBS-0001) and the Gordon and Betty Moore Foundation and NERC Consortium Grants 'AMAZONICA' (NE/F005806/1) who supported the RAINFOR project. O.L.P. is supported by an ERC Advanced Grant and a Royal Society Wolfson Research Merit Award. Finally, we thank the US Geological Survey for providing access to the Landsat data. **Contributions**: BT, MRM and JC designed the study and wrote the paper. BT, MRM, JV and JC analyzed the data. All authors contributed to acquiring the field data and provided input on draft manuscripts. The authors declare no conflict of interest.

494 **References:**

495 Asner, G.P. & Martin, R.E. (2012) Contrasting leaf chemical traits in tropical lianas and trees:
496 implications for future forest composition. Ecology Letters, **15**, 1001–1007.

497 Bongers, F., Charles-Dominique**,** P., Forget, P.-M., Théry, M. (2001) Nouragues: Dynamics and
498 Plant-Animal Interactions in a Neotropical Rainforest. Klüwer Academic Publishers,
499 Dordrecht, The Netherlands.

500 Bonner, M.T., Schmidt, S. & Shoo, L. P. (2013) A meta-analytical global comparison of above-
501 ground biomass accumulation between tropical secondary forests and monoculture
502 plantations. Forest Ecology and Management, **291**, 73-86.

503 Brienen, R. J. W., Phillips, O. L., Feldpausch, T. R., Gloor, E., Baker, T. R., Lloyd, J., G. Lopez-
504 Gonzalez, A. Monteagudo-Mendoza, Y. Malhi, S. L. Lewis, R. Vásquez Martinez, M.
505 Alexiades, E. Álvarez Dávila, P. Alvarez-Loayza, A. Andrade, L. E. O. C. Aragão, A.
506 Araujo-Murakami, E. J. M. M. Arets, L. Arroyo, G. A. Aymard C., O. S. Bánki, C. Baraloto,
507 J. Barroso,D. Bonal, R. G. A. Boot, J. L. C. Camargo, C. V. Castilho, V. Chama, K. J. Chao,
508 J. Chave, J. A. Comiskey, F. Cornejo Valverde, L. da Costa, E. A. de Oliveira, A. Di Fiore,
509 T. L. Erwin, S. Fauset, M. Forsthofer, D. R. Galbraith, E. S. Grahame, N. Groot, B. Hérault,
510 N. Higuchi, E. N. Honorio Coronado, H. Keeling, T. J. Killeen, W. F. Laurance, S.
511 Laurance, J. Licona, W. E. Magnussen, B. S. Marimon, B. H. Marimon-Junior, C. Mendoza,
512 D. A. Neill, E. M. Nogueira,P. Núñez, N. C. Pallqui Camacho, A. Parada, G. Pardo-Molina,
513 J. Peacock, M. Peña-Claros,G. C. Pickavance, N. C. A. Pitman, L. Poorter, A. Prieto, C. A.
514 Quesada, F. Ramírez, H. Ramírez-Angulo, Z. Restrepo, A. Roopsind, A. Rudas, R. P.
515 Salomão, M. Schwarz, N. Silva,J. E. Silva-Espejo, M. Silveira, J. Stropp, J. Talbot, H. ter
516 Steege, J. Teran-Aguilar, J. Terborgh, R. Thomas-Caesar, M. Toledo, M. Torello-Raventos,
517 R. K. Umetsu, G. M. F. van der Heijden, P. van der Hout, I. C. Guimarães Vieira, S. A.
518 Vieira, E. Vilanova, V. A. Vos & R. J. Zagt (2015). Long-term decline of the Amazon
519 carbon sink. Nature, **519** (7543), 344-348.

520

521 Brown, S. & Lugo, A.E. (1990) Tropical secondary forests. Journal of Tropical Ecology, **6**, 1–32.

522 Caballé, G. (1978) Essai sur la géographie forestière du Gabon. Adansonia, **17**, 425–440.

523 Carvalhais, N., Forkel, M., Khomik, M., Bellarby, J., Jung, M., Migliavacca, M., Mu, M., Saatchi,
524 S., Santoro, M., Thurner, M. & others. (2014) Global covariation of carbon turnover times
525 with climate in terrestrial ecosystems. Nature. **514**, 213–217.

526 Chave, J., Navarrete, D., Almeida, S., Alvarez, E., Aragão, L.E., Bonal, D., Châtelet, P., Silva-
527 Espejo, J.E., Goret, J.-Y., Hildebrand, P. von, Jimenez, E., Patiño, S., Peñuela, M.C.,
528 Phillips, O.L., Stevenson, P. & Malhi, Y. (2010) Regional and seasonal patterns of litterfall
529 in tropical South America. Biogeosciences, **7**, 43–55.

530 Chave, J., Olivier, J., Bongers, F., Châtelet, P., Forget, P.-M., van der Meer, P., Norden, N., Riéra,
531 B. & Charles-Dominique, P. (2008) Above-ground biomass and productivity in a rain forest
532 of eastern South America. Journal of Tropical Ecology, **24**, 355–366.

533 Chave, J., Réjou-Méchain, M., Búrquez, A., Chidumayo, E., Colgan, M.S., Delitti, W.B.C., Duque,
534 A., Eid, T., Fearnside, P.M., Goodman, R.C., Henry, M., Martínez-Yrízar, A., Mugasha,
535 W.A., Muller-Landau, H.C., Mencuccini, M., Nelson, B.W., Ngomanda, A., Nogueira,
536 E.M., Ortiz-Malavassi, E., Pélissier, R., Ploton, P., Ryan, C.M., Saldarriaga, J.G. &

Vieilledent, G. (2014) Improved allometric models to estimate the above-ground biomass of tropical trees. Global Change Biology, **20**, 3177–3190.

Chave, J., Riéra, B. & Dubois, M.-A. (2001) Estimation of biomass in a Neotropical forest of French Guiana: spatial and temporal variability. Journal of Tropical Ecology, **17**, 79–96.

Clark, D.A., Brown, S., Kicklighter, D.W., Chambers, J.Q., Thomlinson, J.R. & Ni, J. (2001) Measuring net primary production in forests: concepts and field methods. Ecological Applications, **11**, 356–370.

Clark, D.B. & Clark, D.A. (1990) Distribution and effects on tree growth of lianas and woody hemiepiphytes in a Costa Rican tropical wet forest. Journal of Tropical Ecology, **6**, 321–331.

Coudreau, H. (1893) Chez nos Indiens– Quatre Années dans la Guyane française (1887-1891). Librairie Hachette et Cie, Paris.

Crist, E.P. & Cicone, R.C. (1984) A physically-based transformation of thematic mapper data—The TM tasseled cap. Geoscience and Remote Sensing, IEEE Transactions On, 256–263.

Dalling, J.W. & Hubbell, S.P. (2002) Seed size, growth rate and gap microsite conditions as determinants of recruitment success for pioneer species. Journal of Ecology, **90**, 557–568.

Dalling, J.W., Schnitzer, S.A., Baldeck, C., Harms, K.E., John, R., Mangan, S.A., Lobo, E., Yavitt, J.B. & Hubbell, S.P. (2012) Resource-based habitat associations in a neotropical liana community. Journal of Ecology, **100**, 1174–1182.

Davidson, E.A., de Araújo, A.C., Artaxo, P., Balch, J.K., Brown, I.F., C. Bustamante, M.M., Coe, M.T., DeFries, R.S., Keller, M., Longo, M., Munger, J.W., Schroeder, W., Soares-Filho, B.S., Souza, C.M. & Wofsy, S.C. (2012) The Amazon basin in transition. Nature, **481**, 321–328.

DeWalt, S.J. & Chave, J. (2004) Structure and biomass of four lowland Neotropical forests. Biotropica, **36**, 7–19.

Foster, J.R., Townsend, P.A. & Zganjar, C.E. (2008) Spatial and temporal patterns of gap dominance by low-canopy lianas detected using EO-1 Hyperion and Landsat Thematic Mapper. Remote Sensing of Environment, **112**, 2104–2117.

Granados, J. & Körner, C. (2002) In deep shade, elevated CO2 increases the vigor of tropical climbing plants. Global Change Biology, **8**, 1109–1117.

Guzman-Grajales, S.M. & Walker, L.R. (1991) Differential seedling responses to litter after hurricane Hugo in the Luquillo experimental forest, Puerto Rico. Biotropica, **23**, 407–413.

van der Heijden, G.M.F., Feldpausch, T.R., Herrero, A. de la F., van der Velden, N.K. & Phillips, O.L. (2010) Calibrating the liana crown occupancy index in Amazonian forests. Forest Ecology and Management, **260**, 549–555.

van der Heijden, G.M.F. & Phillips, O.L. (2008) What controls liana success in Neotropical forests? Global Ecology and Biogeography, **17**, 372–383.

van der Heijden, G.M.F. & Phillips, O.L. (2009) Liana infestation impacts tree growth in a lowland tropical moist forest. Biogeosciences, **6**, 2217–2226.

van der Heijden, G.M.F., Schnitzer, S.A., Powers, J.S. & Phillips, O.L. (2013) Liana impacts on carbon cycling, storage and sequestration in tropical forests. Biotropica, **45**, 682–692.

Hendershot, W.H., Lalande, H. & Duquette, M. (1993) Ion exchange and exchangeable cations. Soil Sampling and Methods of Analysis, **19**, 167–176.

Hill, R.A. (1999) Image segmentation for humid tropical forest classification in Landsat TM data. International Journal of Remote Sensing, **20**, 1039–1044.

Hubbell, S.P., Foster, R.B., O'Brien, S.T., Harms, K.E., Condit, R., Wechsler, B., Wright, S.J. & De Lao, S.L. (1999) Light-gap disturbances, recruitment limitation, and tree diversity in a neotropical forest. Science, **283**, 554–557.

Ingwell, L.L., Wright J., S., Becklund, K.K., Hubbell, S.P. & Schnitzer, S.A. (2010) The impact of lianas on 10 years of tree growth and mortality on Barro Colorado Island, Panama. Journal of Ecology, **98**, 879–887.

Lahtinen, R. (2000) Archaean–proterozoic transition: geochemistry, provenance and tectonic setting of metasedimentary rocks in central Fennoscandian shield, Finland. Precambrian Research, **104**, 147–174.

Laurance, W.F., Andrade, A.S., Magrach, A., Camargo, J.L.C., Valsko, J.J., Campbell, M., Fearnside, P.M., Edwards, W., Lovejoy, T.E. & Laurance, S.G. (2014) Long-term changes in liana abundance and forest dynamics in undisturbed Amazonian forests. Ecology, **95**, 1604–1611.

Ledo, A. & Schnitzer, S.A. (2014) Disturbance and clonal reproduction determine liana distribution and maintain liana diversity in a tropical forest. Ecology, **95**, 2169–2178.

Letcher, S.G. & Chazdon, R.L. (2012) Life history traits of lianas during tropical forest succession. Biotropica, **44**, 720–727.

Lopez-Gonzalez, G., Lewis, S.L., Burkitt, M. & Phillips, O.L. (2011) ForestPlots. net: a web application and research tool to manage and analyse tropical forest plot data. Journal of Vegetation Science, **22**, 610–613.

Lozada, J.R., Hernández, C., Soriano, P. & Costa, M. (2015) An assessment of the floristic composition, structure and possible origin of a liana forest in the Guayana Shield. Plant Biosystems -An International Journal Dealing with all Aspects of Plant Biology, **0**, 1–10.

McGaughey, R.J. (2009) FUSION/LDV: Software for LIDAR data analysis and visualization. US Department of Agriculture, Forest Service, Pacific Northwest Research Station: Seattle, WA, USA, **123**.

McLennan, S.M., Hemming, S., McDaniel, D.K. & Hanson, G.N. (1993) Geochemical approaches to sedimentation, provenance, and tectonics. Geological Society of America Special Papers, **284**, 21–40.

Norden, N., Chave, J., Belbenoit, P., Caubère, A., Châtelet, P., Forget, P.-M., Riéra, B., Viers, J. & Thébaud, C. (2009) Interspecific variation in seedling responses to seed limitation and habitat conditions for 14 Neotropical woody species. Journal of Ecology, **97**, 186–197.

Norden, N., Chave, J., Caubère, A., Châtelet, P., Ferroni, N., Forget, P.-M. & Thébaud, C. (2007) Is temporal variation of seedling communities determined by environment or by seed arrival? A test in a Neotropical forest. Journal of Ecology, **95**, 507–516.

Béchamel, F.-J.B. Journal du Voyage que les Pères Jean Grillet et François Béchamel ont Fait dans la Guyane en 1674. Claude Barbin, Paris

Pérez-Salicrup, D.R. (2001) Effect of liana cutting on tree regeneration in a liana forest in Amazonian Bolivia. Ecology, **82**, 389–396.

Phillips, O.L. & Gentry, A.H. (1994) Increasing turnover through time in tropical forests. Science, **263**, 954–958.

Phillips, O.L., Vargas, P.N., Monteagudo, A.L., Cruz, A.P., Zans, M.-E.C., Sánchez, W.G., Yli-Halla, M. & Rose, S. (2003) Habitat association among Amazonian tree species: a landscape-scale approach. Journal of Ecology, **91**, 757–775.

Phillips, O.L., Vásquez Martínez, R., Arroyo, L., Baker, T.R., Killeen, T., Lewis, S.L., Malhi, Y., Monteagudo Mendoza, A., Neill, D., Núñez Vargas, P., Alexiades, M., Cerón, C., Di Fiore, A., Erwin, T., Jardim, A., Palacios, W., Saldias, M. & Vinceti, B. (2002) Increasing dominance of large lianas in Amazonian forests. Nature, **418**, 770–774.

Putz, F.E. (1983) Liana biomass and leaf area of a "tierra firme" forest in the Rio Negro basin, Venezuela. Biotropica, **15**, 185–189.

Putz, F.E. (1984a) The natural history of lianas on Barro Colorado Island, Panama. Ecology, **65**, 1713–1724.

Putz, F.E. (1984b) How trees avoid and shed lianas. Biotropica, **16**, 19–23.

R Core Team. (2012) R: A Language and Environment for Statistical Computing. R Foundation for Statistical Computing, Vienna, Austria.

van der Sande, M.T., Poorter, L., Schnitzer, S.A. & Markesteijn, L. (2013) Are lianas more drought-tolerant than trees? A test for the role of hydraulic architecture and other stem and leaf traits. Oecologia, **172**, 961–972.

Sabatier, D., & Prévost, M. F. (1990) Quelques données sur la composition floristique et la diversité des peuplements forestiers de Guyane française. Bois et Forêts des Tropiques, **219**, 31-55.

Schnitzer, S.A. (2005) A mechanistic explanation for global patterns of liana abundance and distribution. American Naturalist, **166**, 262–276.

Schnitzer, S.A. & Bongers, F. (2002) The ecology of lianas and their role in forests. Trends in Ecology & Evolution, **17**, 223–230.

Schnitzer, S.A. & Bongers, F. (2011) Increasing liana abundance and biomass in tropical forests: emerging patterns and putative mechanisms. Ecology Letters, **14**, 397–406.

Schnitzer, S.A. & Carson, W.P. (2010) Lianas suppress tree regeneration and diversity in treefall gaps. Ecology Letters, **13**, 849–857.

Schnitzer, S.A., Dalling, J.W. & Carson, W.P. (2000) The impact of lianas on tree regeneration in tropical forest canopy gaps: evidence for an alternative pathway of gap-phase regeneration. Journal of Ecology, **88**, 655–666.

Schnitzer, S.A., DeWalt, S.J. & Chave, J. (2006) Censusing and measuring lianas: a quantitative comparison of the common methods. Biotropica, **38**, 581–591.

Schnitzer, S.A., van der Heijden, G., Mascaro, J. & Carson, W.P. (2014) Lianas in gaps reduce carbon accumulation in a tropical forest. Ecology, **95**, 3008–3017.

Schnitzer, S.A., Mangan, S.A., Dalling, J.W., Baldeck, C.A., Hubbell, S.P., Ledo, A., Muller-Landau, H., Tobin, M.F., Aguilar, S., Brassfield, D., Hernandez, A., Lao, S., Perez, R., Valdes, O. & Yorke, S.R. (2012) Liana abundance, diversity, and distribution on Barro Colorado Island, Panama. PLoS ONE, **7**, e52114.

Schwertfeger, D.M. & Hendershot, W.H. (2009) Determination of effective cation exchange capacity and exchange acidity by a one-step BaCl method. Soil Science Society of America Journal, **73**, 737–743.

Sheil, D. & May, R.M. (1996) Mortality and recruitment rate evaluations in heterogeneous tropical forests. Journal of Ecology, **84**, 91–100.

Sollins, P. (1998) Factors influencing species composition in tropical lowland rain forest: does soil matter? Ecology, **79**, 23–30.

Tuomisto, H., Poulsen, A.D., Ruokolainen, K., Moran, R.C., Quintana, C., Celi, J. & Cañas, G. (2003) Linking floristic patterns with soil heterogeneity and satellite imagery in Ecuadorian Amazonia. Ecological Applications, **13**, 352–371.

Turner, B.L. & Romero, T.E. (2009) Short-term changes in extractable inorganic nutrients during storage of tropical rain forest soils. Soil Science Society of America Journal, **73**, 1972.

Vanderhaeghe, O., Ledru, P., Thiéblemont, D., Egal, E., Cocherie, A., Tegyey, M. & Milési, J.-P. (1998) Contrasting mechanism of crustal growth: Geodynamic evolution of the Paleoproterozoic granite–greenstone belts of French Guiana. Precambrian Research, **92**, 165–193.

Wright, S.J., Calderón, O., Hernandéz, A. & Paton, S. (2004) Are lianas increasing in importance in tropical forests? A 17-year record from Panama. Ecology, **85**, 484–489

SUPPORTING INFORMATION

Appendix S1: Quantification of liana infestation in tree crowns

Appendix S2: Impact of liana infestation on individual tree growth

Appendix S3: Soil analyses

Appendix S4: Airborne LiDAR data acquisition processing, and analyses

Figure S1: Crown occupation index (COI).

Figure S2: Size class distribution of trees in 2012.

Figure S3: Principal Component Analysis (PCA) performed on the tasseled-cap indices of the 2006 Landsat image.

Figure S4: PCA of the chemical tracers in rocks of the Guiana Shield and in the available soil sample.

Figure S5: Total soil composition below the different forest types.

Figure S6: Available elements composition of the soil below the different forest types.

Figure S7: Changes of above-ground biomass stocks in the study area between 1992 and 2012.

Table S1: Chemical composition in trace elements of the fraction of soil sample < 2 mm.

Tables

Table 1: Demography, AGB stock and dynamics across forest types. Canopy metrics were computed from a 1-m resolution LiDAR canopy model in 50x50m² subplots, 332 of which were in high-canopy forest and 93 in liana-infested forest. Tree demography was inferred from 25x25 m² subplots, 87 in high-canopy forest and 17 in liana-infested forest. Litterfall was measured from 100 litterfall traps of 0.5 m², 62 in high-canopy forest and eight in the liana-infested forest. Average values ± standard error are reported. Pairwise comparisons between high-canopy forest and liana-infested forest are reported throughout the table (two-sided Wilcoxon test adjusted by Bonferroni correction, - p>0.0.5, * p≤0.05, ** p≤0.01, *** p≤0.001).

Table 2: Comparison of seedling dynamics across forest types. Average values ± standard errors are provided. Tree and liana seedlings were monitored in 247 plots of 1x1m² at 1.5m of the litterfall traps (see Table 1).Results are also reported for all seedlings including undetermined (total). Pairwise comparisons between high-canopy forest and liana-infested forest are reported throughout the table (two-sided Wilcoxon test adjusted by Bonferroni correction, - p>0.05, * p≤0.05, ** p≤0.01, *** p≤0.001). Average values ± standard error are reported.

Table 3: Comparison of soil characteristics across forest types. Results of a complete digestion of the soil (Total soil content) and a chemical extraction (Soil exchangeable elements) analyses are presented here. All results are reported in ppm unless specified otherwise. Pairwise tests between high-canopy forest and liana-infested forest were performed only on PCA axis and Base saturation values (two-sided Wilcoxon test adjusted by Bonferroni correction, - p>0.05, * p≤0.05, *** p≤0.001).

717 **Table 1**

Variable	High-canopy forest	Liana-infested forest	Significance
Structural variables			
Mean tree density (ha^{-1})	486±5	482±10	-
Mean basal area (m^2 ha^{-1})	29.4±0.6	17.6±0.7	***
Top canopy height (m)	30.4±0.2	16.5±0.28	***
Mean canopy height (m)	31.3±0.5	18.6±0.8	***
CV of canopy height (m)	0.29±0	0.5±0	***
Tree trunk AGB stock (Mg ha^{-1})	414±13	172±10	***
Liana AGB stock (Mg ha^{-1})	2.89±0.45	2.93±0.66	*
New gaps in 2012 from 2007 (m^2 ha^{-1})	140±11.6	500±48	***
Demographics (in % $year^{-1}$)			
Canopy height change	-0.42±0.1	-0.28±0.16	-
Tree diameter growth rate	0.79±0.01	0.93±0.01	-
Tree mortality rate	1.51±0.09	3.03±0.36	***
Tree recruitment rate	1.4±0.1	2.93±0.37	***
AGB dynamics (in Mg ha^{-1} $year^{-1}$)			
Mortality-induced loss of ABG	4.95±0.69	5.48±0.52	-
Recruitment-induced AGB gain	0.34±0.03	0.77±0.06	**
Growth-induced AGB gain	7.28±0.31	3.77±0.14	**
Net tree AGB change	2.66±0.81	-0.94±0.56	*
Net liana AGB change	0.12±0.08	0.17±0.09	*
Leaf litterfall	6.2±1.6	7.5±1.3	*
Flower litterfall	0.2±0.33	0.14±0.21	-
Fruit litterfall	0.52±0.46	0.12±0.07	***
Twigs litterfall	2±1.3	2.56±1.66	-
Total litterfall	8.9±2.29	10.4±2.27	-
Net primary productivity	16.5	14.9	
Carbon residence time (year)	25.2	11.7	

718

719 **Table 2**

Seedling variables	High-canopy forest	Liana-infested forest	Significance
Seedling density (m^{-2})	17.3±0.7	7.8±0.7	***
Proportion of lianas (%)	23±1	25±5	-
Seedling mortality (% $year^{-1}$)			
Trees	12.9±0.7	13.6±2.3	-
Lianas	12.4±1.2	13.9±3.7	-
Total	19.3±0.7	26.7±3.1	*
Seedling recruitment ($year^{-1}$)			
Trees	1.75±0.2	0.71±0.11	***
Lianas	0.85±0.15	0.95±0.47	-
Total	3.54±0.25	2.07±0.28	**

720

721 **Table 3**

	High canopy forest	Liana infested forest	Difference
Total soil composition (ppm)			
Al	38.9±0.64	35.48±1.1	
Ca	0.09±0.01	0.24±0.03	
K	0.09±0.01	0.1±0.04	
Fe	46.5±0.68	52.94±2.29	
Mg	0.14±0	0.17±0.02	
Na	-0.05±0	0±0.01	
N	0.29±0.01	0.34±0.03	
C	3.48±0.13	3.5±0.36	
pH	4.83±0.04	5.33±0.11	
PCA axis 1	-0.5±0.18	0.66±0.75	*
PCA axis 2	-0.4±0.15	1.42±0.43	***
Soil exchangeable elements(ppm)			
P	0.3±0.05	0.37±0.1	
Fe	0.41±0.12	0.24±0.16	
Al	108±11.3	58±21.3	
Ca	179±28	322±79.7	
K	27.31±9.85	31.43±15.52	
Mg	45.64±5.73	88.73±20.16	
Mn	11.32±1.41	14.05±2.66	
Na	5.43±0.98	4.71±1.77	
pH	4.28±0.03	4.41±0.1	
TEB (cmolc kg^{-1})	1.36±0.19	2.44±0.53	
ECEC (cmolc kg^{-1})	2.66±0.17	3.2±0.37	
Base saturation (%)	0.71±0.04	0.89±0.08	*
PCA axis 1	0.84±0.33	-1.16±1.02	*
PCA axis 2	-0.09±0.35	0.07±0.63	-

722

Figure captions

Figure 1: Map of the study area. Panel a: LiDAR-derived canopy height model for a 2000-ha area of the Nouragues Ecological Research Station; panel b: enhancement of panel a, zooming in the focal study area of 136 ha; panel c: aerial photography of the focal study area. Thick dashed line: zone of interest, thin dashed line: permanent plots, thin solid line: liana forest, and transition zone (thick solid line) in 2007. In white: zone removed from analyses (bamboo thicket). Black triangles in panel b show the site where soil was collected for trace element analysis (panel b). Circles in panel c indicate places where soil was collected for complete digestion (red) or partial digestion (yellow). Red points also indicate positions of litterfall traps and seedling monitoring plots. Black rectangle on panel c shows the position of the transect shown as an example in figure 2.

Figure 2: Transition from liana-infested to high-canopy forest. Panels a and b: photography of the liana-infested forest and of the high forest taken from the top of the neighbouring granitic outcrop (inselberg). Panels c and d: Three dimension view of the canopy model (top of canopy height) of two 64x64 m² areas in (c) and out (d) of the liana-infested forest. Panel e: Height of the canopy model in a 20x500 m² transect. Two dashed lines are drawn at the median canopy top height in each formation (16.5 and 30.4 m). Canopy gaps are defined by a top canopy height below 5m (dotted lines). Position of the transect is shown Fig.1.

Figure 3: Ratios of trace elements. Averages were calculated for liana-infested and high-canopy forest soil samples. Values were divided by the average value for all measured points (value on the left for each graphics) giving the relative plotted values. These ratios were compared to literature values for rocks present in French Guiana (open symbols ; (Vanderhaeghe et al. 1998)). Values on the left side of each graphics are averages for all soil samples.

Figure 4: Spatial dynamics of the liana-infested forest. Landsat-derived maps of vegetation, obtained by a unsupervised hierarchical classification (see Methods). The class 4 can be conservatively identified to the liana-infested forest (88% accuracy, 72% precision). Solid line represents the extent of the liana-infested forest as defined from the 2007 LiDAR canopy model (with the transition zone shown as a dotted line, see Fig. 1). The bamboo thicket was removed from the classification (area masked in white).

Figures:

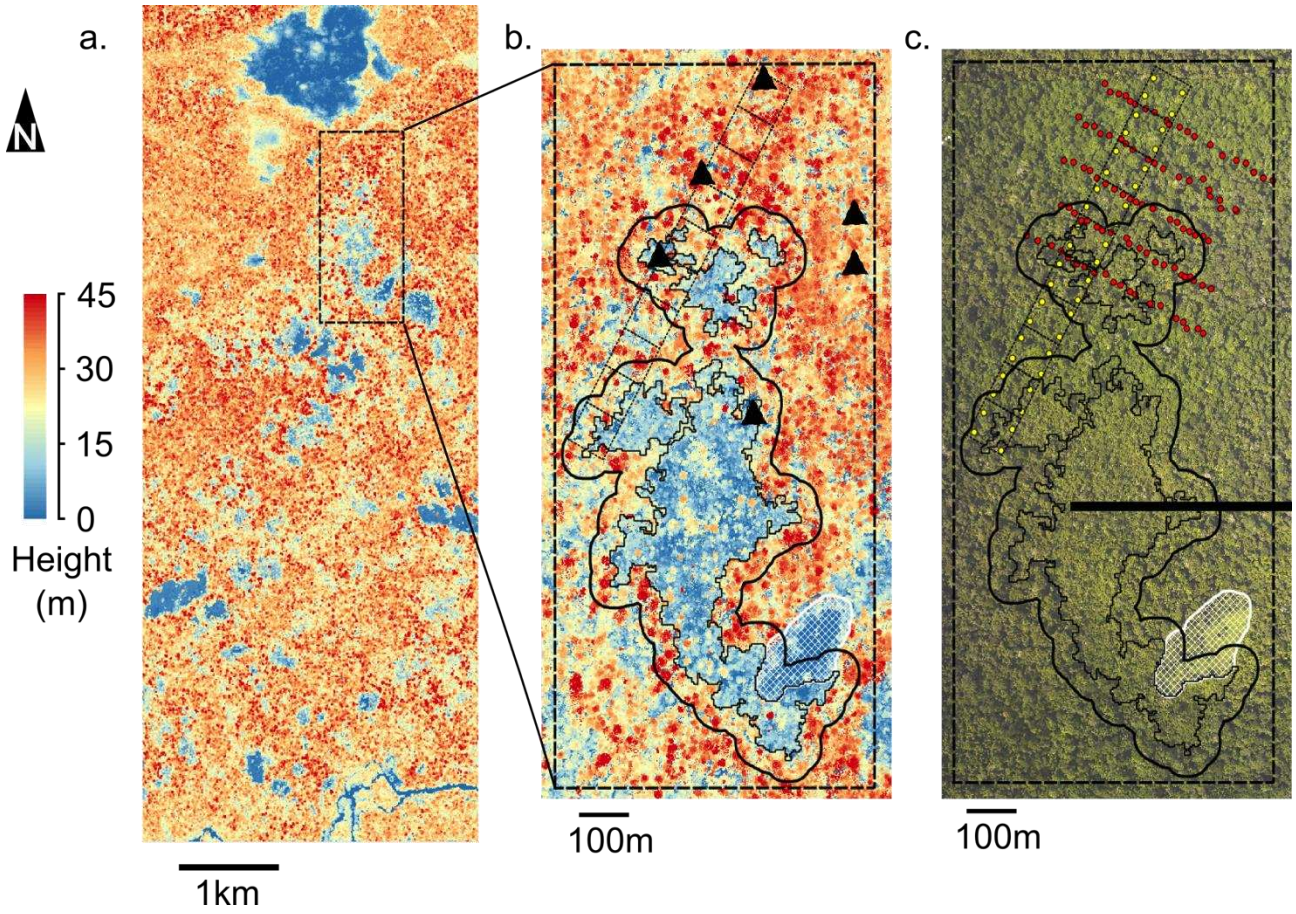

Figure 1

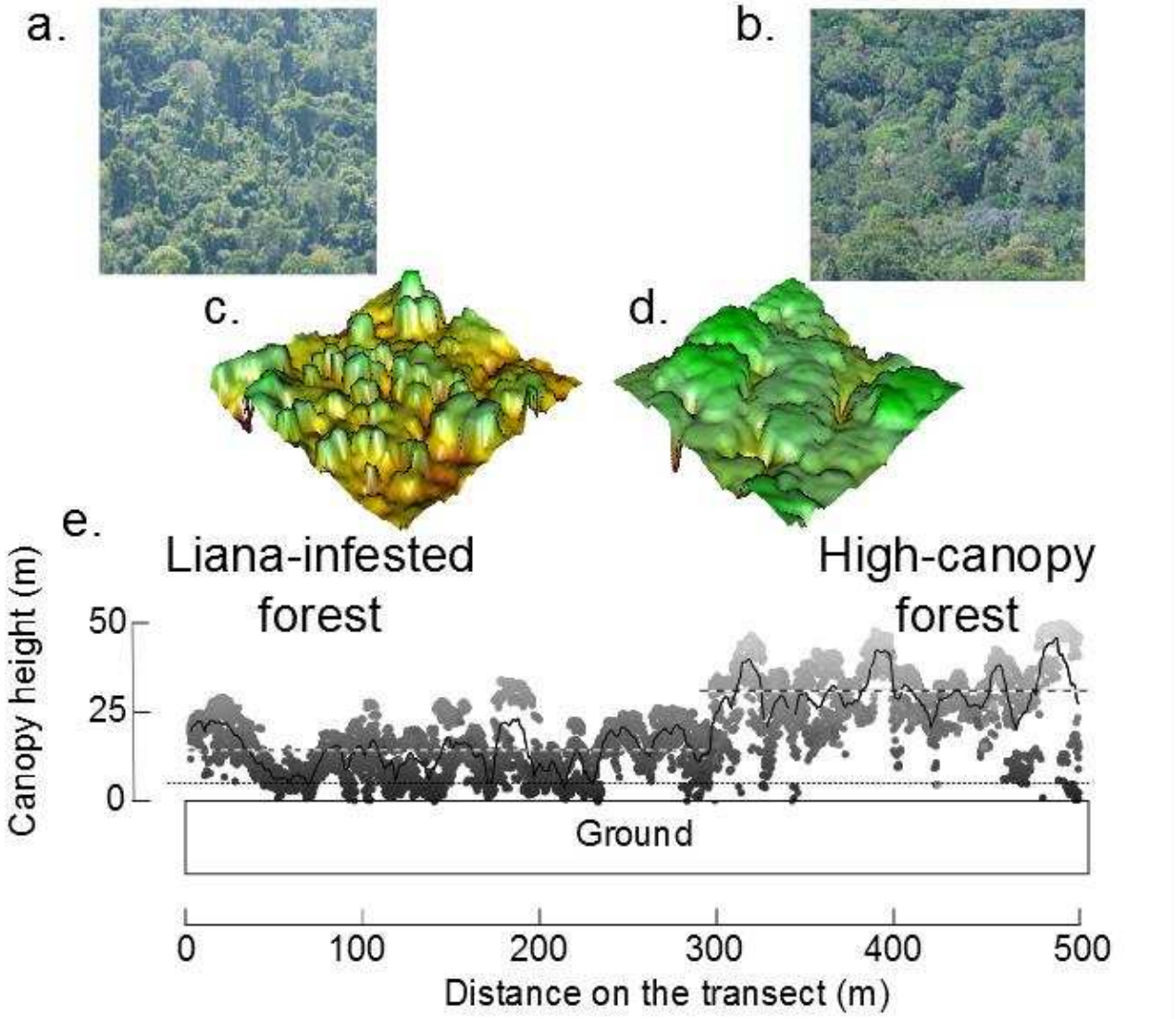
a.
b.
c.
d.
e.
Liana-infested forest
High-canopy forest
Canopy height (m)
50
25
0
Ground
0
100
200
300
400
500
Distance on the transect (m)

Figure 2

757

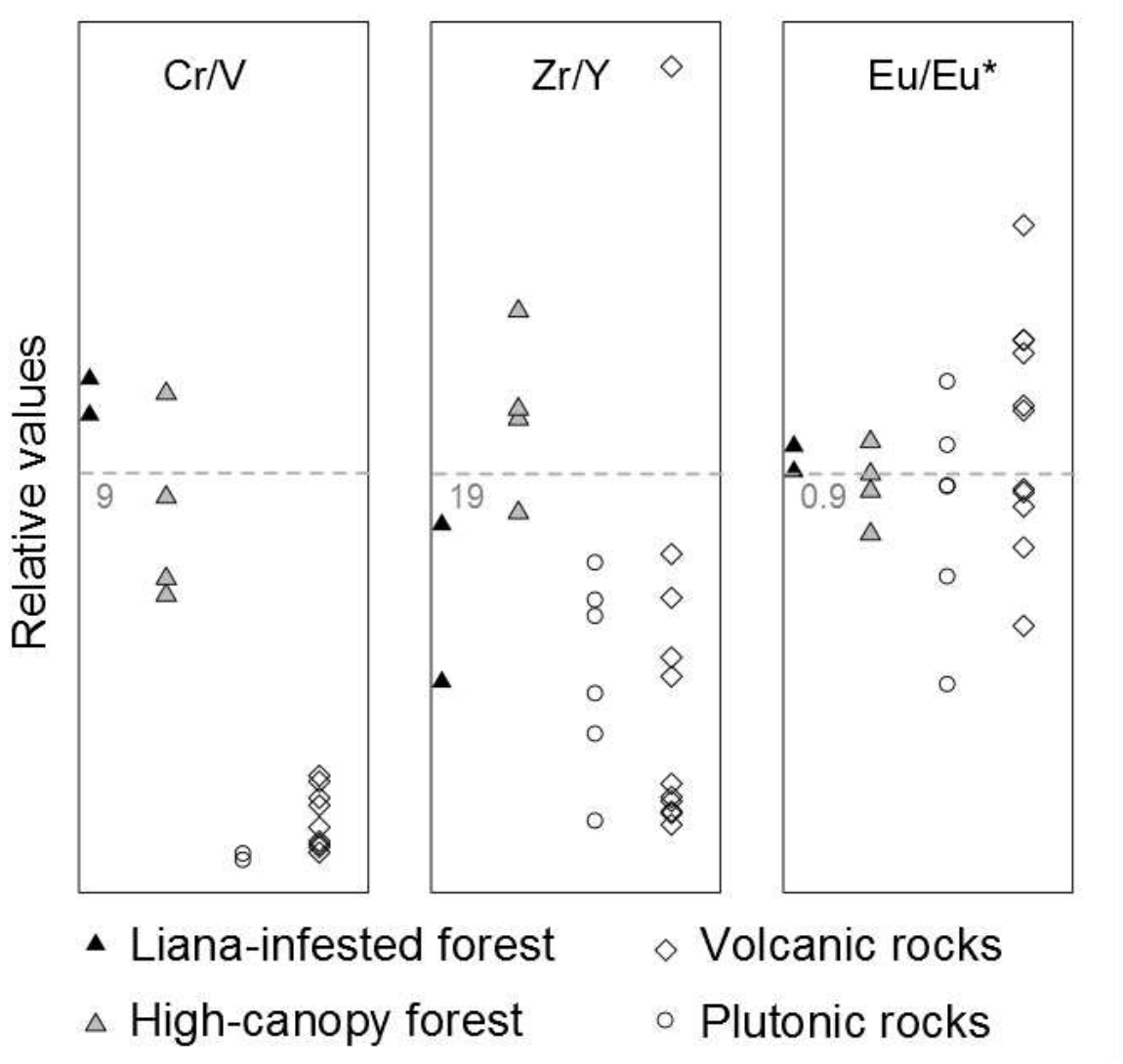

758

759 **Figure 3**

760

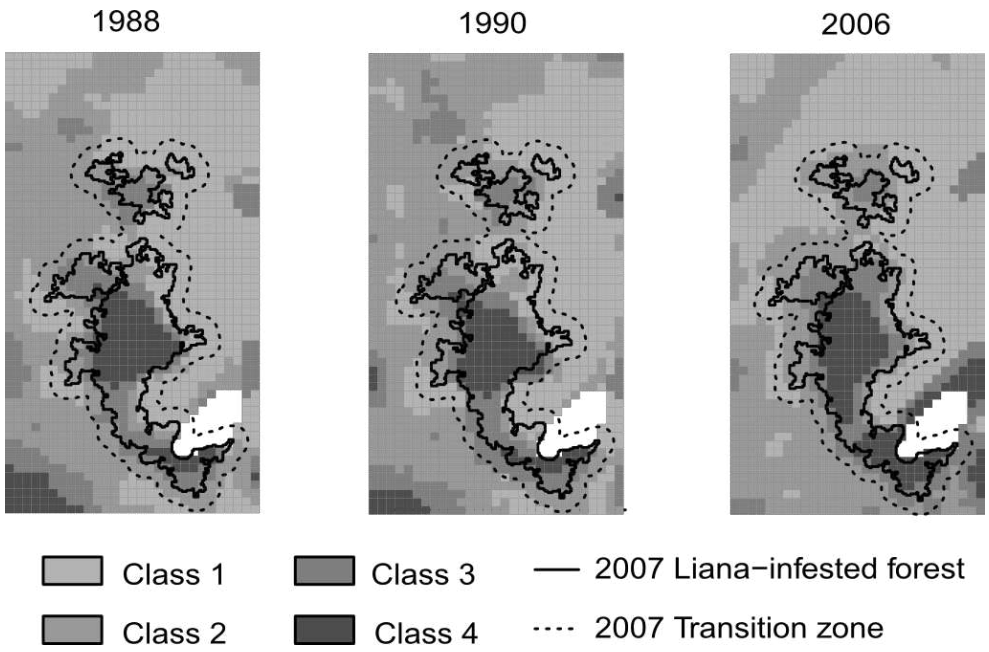

761

Figure 4

762

763